

Variational Bayes for Federated Continual Learning

Dezhong Yao, Sanmu Li, Yutong Dai, Zhiqiang Xu, Shengshan Hu, Peilin Zhao, and Lichao Sun

Abstract—Federated continual learning (FCL) has received increasing attention due to its potential in handling real-world streaming data, characterized by evolving data distributions and varying client classes over time. The constraints of storage limitations and privacy concerns confine local models to exclusively access the present data within each learning cycle. Consequently, this restriction induces performance degradation in model training on previous data, termed “catastrophic forgetting”. However, existing FCL approaches need to identify or know changes in data distribution, which is difficult in the real world. To release these limitations, this paper directs attention to a broader continuous framework. Within this framework, we introduce Federated Bayesian Neural Network (FedBNN), a versatile and efficacious framework employing a variational Bayesian neural network across all clients. Our method continually integrates knowledge from local and historical data distributions into a single model, adeptly learning from new data distributions while retaining performance on historical distributions. We rigorously evaluate FedBNN’s performance against prevalent methods in federated learning and continual learning using various metrics. Experimental analyses across diverse datasets demonstrate that FedBNN achieves state-of-the-art results in mitigating forgetting.

Index Terms—Federated learning, continual learning, catastrophic forgetting, variational inference, privacy preservation.

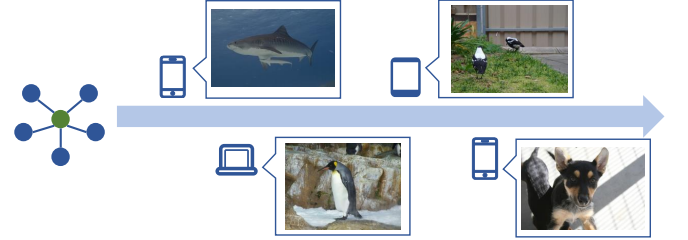
I. INTRODUCTION

FEDERATED Learning (FL) facilitates collaborative training of a global model among mobile devices or small-scale organizations, effectively overcoming data silos and data privacy challenges [1], [2]. Serving as a communication-efficient and privacy-preserving training scheme, FL has been widely used in various applications, such as keyboard prediction [3], [4], medical diagnosis [5], autonomous driving [6], and object detection [7], [8].

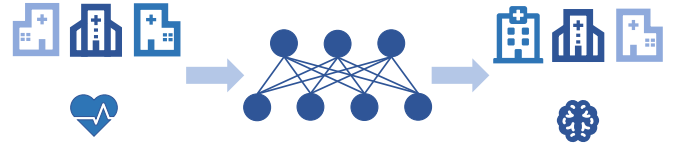
However, traditional FL algorithms operate under the assumption that data distribution and classes remain constant across all devices. Real-world scenarios, however, witness clients continually encountering new concepts and evolving data distribution over time [9], [10]. As illustrated in Fig. 1, instances such as the emergence of new object detection classes reported by individual users (Fig. 1a), or the application of a federated diagnostic system to a new department within a healthcare institute (Fig. 1b), exemplify the evolving nature

Dezhong Yao, Sanmu Li, and Shengshan Hu are with the National Engineering Research Center for Big Data Technology and System, Services Computing Technology and System Lab, Cluster and Grid Computing Lab, School of Computer Science and Technology, Huazhong University of Science and Technology, Wuhan 430074, China (E-mail: {dyao, ltw_cgcl, hushengshan}@hust.edu.cn). Yutong Dai and Lichao Sun are with Lehigh University, PA 18015, USA (E-mail: {yud319, lis221}@lehigh.edu). Zhiqiang Xu is with Mohamed bin Zayed University of Artificial Intelligence, UAE (E-mail: zhiqiang.xu@mbzuai.ac.ae). Peilin Zhao is with Tencent AI Lab, Shenzhen, China. (E-mail: masonzhao@tencent.com)

(Corresponding author: Dezhong Yao), Under review.



(a) Federated class-incremental: users report new classes in a federated object detection system.



(b) Federated task-incremental: a federated diagnosis system switch from the cardiology task to the neurology task.

Fig. 1: In many real world scenarios, the data distribution of a federated learning system will evolve over time [14]. Therefore, approaches that deal with dynamic data distribution are desirable for federated learning systems.

of data. Local clients, constrained by limited storage and privacy considerations, typically retain recent data, granting local models access solely to current data during new learning cycles. This leads to two problems: 1) rapid adaptation of local models to recent classes results in significant degradation in performance on previously learned distribution, known as the *catastrophic forgetting* [11], [12], and 2) a set of local models in FL exhibit performance drop on disparate tasks, referred to as the *negative knowledge transfer* [13]. These challenges render the use of conventional FL in a continual setting inefficient. This motivates us to extend the conventional FL to deal with the federated continual tasks that follow a non-stationary distribution, so we can dynamically update the model to effectively exchange knowledge while avoiding forgetting.

Recently, some efforts have been made to solve federated continual learning challenges stemming from non-stationary distribution. For example, online learning methods [15], [14] minimize the accumulative loss from the perspective of regret minimization. These algorithms require buffering previous data for training, which may be unrealistic as the size of datasets often prohibits frequent batch updating. Also, continual-learning-based approaches [16], [9] avoid revisiting previous data and aim to overcome catastrophic forgetting. These approaches require identification [9] or awareness of data distribution changes [16], which is also unrealistic when there is no clear task boundary.

In this paper, we propose a Bayesian neural network (BNN)

based approach, named **FedBNN**¹, which tackles the issues of negative knowledge transfer and catastrophic forgetting for general FCL tasks. By integrating knowledge of previous data into the BNN prior and properly aggregating locally learned BNN distributions, FedBNN demonstrates the capability to sustain its performance on past data distributions while continually learning from new distributions, despite the data heterogeneity among clients. Remarkably, the proposed approach is task-agnostic by nature and can be applied to the general FCL problem. It is empirically shown that the Bayesian formulation of our algorithm effectively alleviates negative transfer among different tasks to overcome the catastrophic forgetting issue.

Summary of Contributions:

- We formulate a comprehensive definition of FCL, including both class-incremental and task-incremental scenarios, which do not require clear task boundaries.
- We propose FedBNN, the first variational-based FCL method, to the best of our knowledge. Unlike the previous works, FedBNN can handle FCL without obvious task boundaries.
- We verify the effectiveness of our proposed method over existing baselines via extensive experiments on various FCL settings.

II. BACKGROUNDS

A. Related Work

Continual Learning tries to train a single model that can learn from multiple tasks sequentially [17], [18], [19], [20]. Previous works can be categorized in terms of the continual learning setting as follows: class-incremental learning, task-incremental learning, and domain-incremental learning. Many practical approaches have been proposed to deal with specific settings, like iCaRL [21], EWC [22], and LwF [23]. These settings assume there are well-defined boundaries between tasks, and many of them require the boundary known to the algorithm. However, recent advances introduce task-agnostic continual learning, which dispenses with the need for clear task boundary, and assumes task transitions happen gradually [24], [25]. This is a more realistic and general setting of dynamic learning tasks. In this study, we adopt this setting, reflecting the evolving nature of learning tasks over time.

Federated Continual Learning has emerged to learn new tasks continuously while tackling forgetting on old tasks in federated scenarios [26], [27]. Some approaches have been proposed to learn a global continual model among clients. CFed [28] overcomes catastrophic forgetting on clients by knowledge distillation. FCIL [9], [29] focuses on federated class-incremental settings, addressing catastrophic forgetting by mitigating the imbalance in sample classes. FISS [30] targets the specific application of federated incremental semantic segmentation via adaptive class-balanced pseudo labeling. Notably, these approaches require identifying or knowing changes in data distribution, which is unrealistic in many real-world scenarios. Another series of work focuses on helping each client continuously learn its local model with indirect

knowledge from other clients. FedWEIT [16] achieves this objective by decomposing the model into global parameters and task-specific parameters. FedKNOW [31] further enhances communication efficiency over FedWEIT by storing more lightweight signature knowledge for each local task. In this paper, we still focus on learning a global continual model, since a global model is desirable in prediction on server and newly joined clients [32], [33].

Bayesian Neural Network provides a novel probabilistic perspective of neural networks [34], [35]. It views network parameters as random variables and solves for the posterior distribution of the parameters. Many approaches have been proposed to obtain the posterior distribution, including Expectation Propagation (EP) [36], [37], Variational Inference (VI) [35], [38], [39], and Markov Chain Monte Carlo (MCMC) [40], [41], [42]. Recently, BNN-based approaches have been used in FL [43], [44], [45] and CL [46], [47], [48], and show promising results in solving specific challenges in FL and CL scenarios.

B. Preliminary: BNN and VCL

Bayesian Neural Network (BNN) is an extension of a standard neural network by incorporating Bayesian principles. In BNN, the parameters are treated as random variables. Therefore, instead of a single value, model parameters θ in BNN are modeled by some distribution $p(\theta)$. Given a dataset \mathcal{D} , the fundamental objective in BNN learning is to find the conditional distribution of model parameters on given data $p(\theta|\mathcal{D})$, known as the posterior. Specifically, the Bayes rule is applied:

$$p(\theta|\mathcal{D}) = \frac{p(\theta)p(\mathcal{D}|\theta)}{p(\mathcal{D})} \propto p(\theta)p(\mathcal{D}|\theta) \quad (1)$$

The first term is a prior distribution for the parameter, while the latter is the data-related likelihood. This distribution is intractable itself, but it is viable to approximate it by some parameterized distribution families $q(Z)$, known as variational inference. The notable work of Bayes by Backprop [35] enables efficient inference on large BNNs. It uses mean-field Gaussian distribution as the variational distribution, and makes the approximation via backpropagation and gradient descent, in a manner similar to standard neural networks.

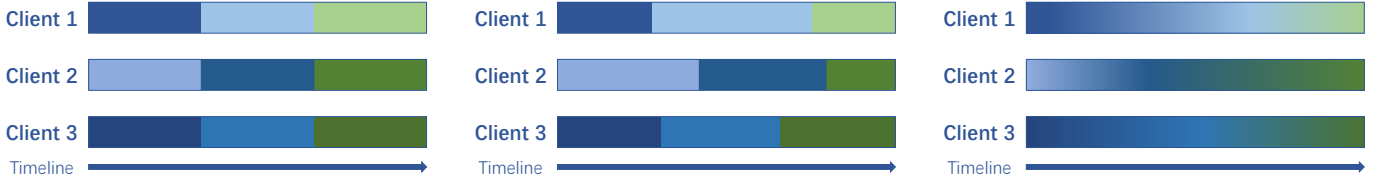
Given the above property of BNN, Variational Continual Learning (VCL) [46] was proposed to address the challenge of continual learning. After a sequence of tasks $\mathcal{D}_{1..T} = \{\mathcal{D}_1, \mathcal{D}_2, \dots, \mathcal{D}_T\}$, the desired parameter distribution $p(\theta|\mathcal{D}_{1..T})$ can be factorized as follows.

$$p(\theta|\mathcal{D}_{1..T}) \propto p(\theta)p(\mathcal{D}_{1..T}|\theta) \quad (2)$$

It is assumed that the dataset samples are conditional independent given parameter θ , so the probability $p(\mathcal{D}_{1..T}|\theta)$ is multiplicative, i.e.

$$p(\mathcal{D}_{1..T}|\theta) = \prod_{t=1}^T p(\mathcal{D}_t|\theta) \quad (3)$$

¹The source code is available at https://github.com/LasSino/fedbnn_code.



(a) All clients change to a new distribution simultaneously. Note the heterogeneity among clients on the same task.

(b) Some clients change to a new distribution ahead of others.

(c) Distribution on each client drifts gradually at different speed.

Fig. 2: In real world FCL applications, data evolution on clients can exhibit different patterns. The figure demonstrates three typical cases of FCL data distribution. Difference of data distribution is demonstrated by different colors.

Therefore, the following recurrence relation holds:

$$\begin{aligned}
 p(\theta|\mathcal{D}_{1..T}) &\propto p(\theta) \prod_{t=1}^T p(\mathcal{D}_t|\theta) \\
 &\propto p(\theta|\mathcal{D}_{1..T-1})p(\mathcal{D}_T|\theta)
 \end{aligned} \quad (4)$$

VCL utilizes the relation to address the problem of continual learning. When a new task is encountered, a new posterior is obtained by setting the latest posterior as the prior and then performing variational inference on the new task. Consequently, the new posterior integrates knowledge about past tasks while learning from the new task, thus robust to distribution change in task shifts.

The success of VCL offers valuable insight into BNN's capacity to integrate knowledge of multiple data distributions into a single model adaptively and continuously. Therefore, employing BNN can be a viable approach to address the FCL problem.

III. PROBLEM FORMULATION OF FCL

It is complicated for multiple clients to collaboratively train a global model from dynamic data streams. To better understand the federated continual learning problem, we first analyze the three main characteristics of real-world FCL scenarios. Based on the analysis, we propose a generalized problem definition that closely fits real-world cases.

A. Motivation: Real World FCL Scenarios

Firstly, FCL systems are expected to operate over extended periods of time, during which the client data evolves. In addition, since training data are generated locally by clients, FCL also needs to handle heterogeneous data among clients (known as the non-IID problem). The primary objective of FCL is to collaboratively train a global model that continuously learns from new data on clients while preserving its performance on previous data distribution.

Secondly, the task boundary of the data stream on each client is unknown, and the data evolution among clients can exhibit various patterns. Fig. 2 illustrates three potential cases of FCL data distribution. In the first case Fig. 2a, the whole FCL system may change its learning data simultaneously and instantly. Alternatively, in the second case Fig. 2b, some clients experience data distribution change before others. Finally, the third case Fig. 2c demonstrates a gradual drift in client distributions over time, each progressing at a distinct rate. This asymmetric evolution of data distribution is commonly

observed in large-scale FCL scenarios. It is important to note that there are typically *no clear task boundaries* during this evolution process, and even if such boundaries exist, they often remain undisclosed to the learning system [24].

Thirdly, while the distribution changes occur separately for each client, we make the assumption that there is a *global trend* followed by the drift in client distributions. This assumption forms the prerequisite for FCL systems. If the distribution drift among clients diverges significantly, collaborative learning among the clients becomes ineffective, rendering FCL approaches unsuitable. Fortunately, this assumption is generally satisfied since trending is a prevalent social phenomenon.

In summary, under real-world FCL scenarios, we need an approach that (1) deals with distributed and evolving data distribution, (2) can be applied to various FCL cases, and (3) is task-agnostic by nature.

B. Problem Definition

General Federated Continual Learning: Suppose K clients collaborate to train a machine learning model, parameterized by θ . Each client k works on its local stream data, and at time t , the local data samples (X, Y) follow some distribution $(X, Y) \sim \mathcal{D}_k^t$. At time t , distributions on clients are different from each other: $\exists k_1 \neq k_2 : \mathcal{D}_{k_1}^t \neq \mathcal{D}_{k_2}^t$. Meanwhile, distribution on the same client will change over time: $\exists t_1 \neq t_2 : \mathcal{D}_k^{t_1} \neq \mathcal{D}_k^{t_2}$.

Although client data is always stored locally, at time t , all clients' data forms a global distribution $\bigcup_k \mathcal{D}_k^t = \mathcal{D}^t$. Due to the evolution of client data, the global distribution is also dynamic: $\exists t_1 \neq t_2 : \mathcal{D}^{t_1} \neq \mathcal{D}^{t_2}$.

At the time t , only a batch of local data from the current distribution \mathcal{D}_k^t is accessible to client k . The goal of FCL is to learn a new global parameter θ^t based on the latest global parameter θ^{t-1} that minimizes loss on all the historical distributions. The objective function at time t_c can be expressed as:

$$\theta^{t_c} = \arg \min_{\theta} \sum_{t=0}^{t_c} \mathcal{L}(\theta; \mathcal{D}^t) = \arg \min_{\theta} \mathcal{L}(\theta; \mathcal{D}^{1..t_c}) \quad (5)$$

where $\mathcal{L}(\theta; \mathcal{D})$ is the loss function on data distribution \mathcal{D} .

This formulation characterizes the client heterogeneity and temporal dynamic of the FCL problem, aiming to learn a model that minimizes the loss of all past data. This formulation is general enough for various real-world scenarios, encompassing the range of cases discussed earlier.

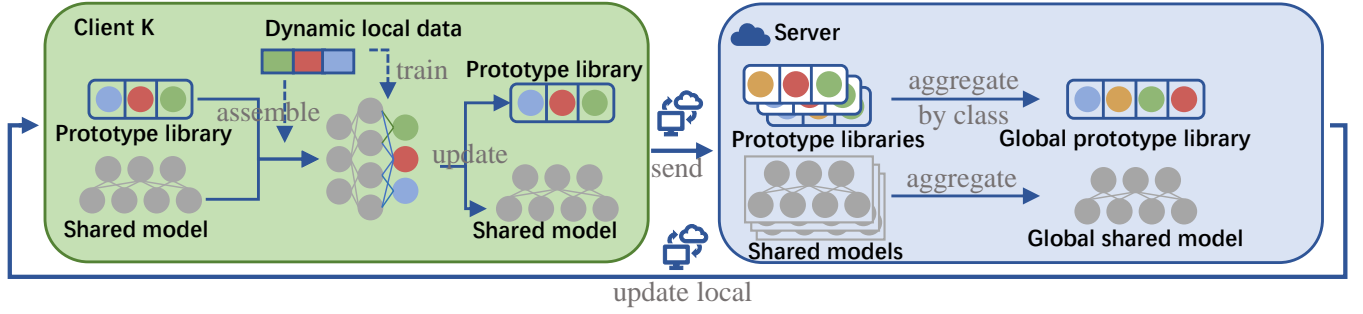


Fig. 3: The mechanism of prototype library in FedBNN. Before local training, the classifier layer is assembled according to classes of current local data. The classifier layer is appended to the shared model for training. After training, the prototypes in the classifier layer are used to update the local prototype library. Local prototype libraries are sent and aggregated by class on the server, then sent back to clients.

IV. THE PROPOSED FEDBNN APPROACH

To deal with dynamic and heterogeneous data streams in FCL, we propose FedBNN. Based on Bayesian Neural Network, our approach is designed to work with the general FCL problem in the real world.

A. Federated Bayesian Neural Network

Inspired by BNN's potential in learning continuously from evolving data distribution, we propose to address the problem of federated continual learning by utilizing a Bayesian neural network. However, the distributed nature of data across numerous clients, coupled with the continual evolution of data distributions among these clients, renders direct learning of a global BNN model unfeasible within the context of FCL. To overcome the challenge of FCL, we propose a novel approach named FedBNN.

Similar to typical FL approaches, the proposed FedBNN operates through iterative communication rounds, during which participating clients cooperate with the server to learn a global model. Within each communication round, FedBNN involves three primary steps to learn a global model: (1) **history-aware local inference**, (2) **local likelihood extraction** and (3) **global knowledge integration**. After one communication round, a global BNN model is learned, which integrates historical knowledge accumulated from both current and previous rounds. The posterior of the global BNN model after communication round T can be denoted as:

$$p(\theta|\mathcal{D}^{1..T}) = p(\theta|\mathcal{D}^{1..T-1} \cup \mathcal{D}^T). \quad (6)$$

History-aware local inference At the start of communication round T , clients receive the latest global model of the last round: $p(\theta|\mathcal{D}^{1..T-1})$. Meanwhile, local data distribution on clients evolves into \mathcal{D}^T . To integrate the new local distribution into the BNN posterior, we perform variational inference locally via Bayes by Backprop:

$$p(\theta|\mathcal{D}^{1..T-1} \cup \mathcal{D}_k^T) \propto p(\theta|\mathcal{D}^{1..T-1})p(\mathcal{D}_k^T|\theta). \quad (7)$$

After local inference, the local model adaptively learns from the latest local distribution and still retains knowledge about historical distributions.

Local likelihood extraction Local inference directly optimizes the approximate posterior $p(\theta|\mathcal{D}^{1..T-1} \cup \mathcal{D}_k^T)$, and

does not explicitly solve for the likelihood $p(\mathcal{D}_k^T|\theta)$. In order to integrate separate local models into a global model, we extract local likelihood from local posterior. By rewriting Eq. (7), the following relation holds:

$$p(\mathcal{D}_k^T|\theta) \propto \frac{p(\theta|\mathcal{D}^{1..T-1} \cup \mathcal{D}_k^T)}{p(\theta|\mathcal{D}^{1..T-1})}. \quad (8)$$

Since the numerator and denominator are both Gaussian distributions, the quotient is also a Gaussian distribution with a constant factor². Therefore, we can represent the local likelihood $p(\mathcal{D}_k^T|\theta)$ by another Gaussian distribution.

Intuitively, local likelihood encapsulates knowledge about the latest local data distribution. After extraction, local likelihoods on clients are sent to the server.

Global knowledge integration With local likelihoods and posterior of the last round, a global model is aggregated on the server. Similar to Eq. (3) in VCL, the global distribution can be decomposed as:

$$\begin{aligned} p(\theta|\mathcal{D}^{1..T-1} \cup \mathcal{D}^T) &\propto p(\theta|\mathcal{D}^{1..T-1})p(\mathcal{D}^T|\theta) \\ &\propto p(\theta|\mathcal{D}^{1..T-1}) \prod_1^k p(\mathcal{D}_k^T|\theta). \end{aligned} \quad (9)$$

With Eq. (9), we can calculate the global posterior on the server, which is a product of multiple Gaussian densities and can be calculated in a closed form. The resulting global posterior $p(\theta|\mathcal{D}^{1..T-1} \cup \mathcal{D}^T)$ integrates knowledge of all the clients over all previous rounds and is used for training in the next round.

Upon completion of a round of FedBNN training, the latest local distributions separate on clients are integrated into the global BNN model, along with historical knowledge. Notably, since FedBNN continuously integrates the latest data distribution during each round, no explicit task boundary is required, making FedBNN applicable to all kinds of FCL scenarios.

B. Prototype Library for Dynamic Label Space

As a particular case of distribution change, new categories may emerge during the learning process. In a neural network,

²Specifically, the following identity holds: $\frac{\mathcal{N}(\mu_1, \Sigma_1)}{\mathcal{N}(\mu_2, \Sigma_2)} \propto \mathcal{N}(\mu, \Sigma)$, where $\Sigma = (\Sigma_1^{-1} - \Sigma_2^{-1})^{-1}$, $\mu = (\Sigma_1^{-1}\mu_1 - \Sigma_2^{-1}\mu_2)\Sigma$.

individual neurons in the output layer correspond to distinct categories in the label space. Thus, new categories cannot be handled by a model with static architecture. In some CL approaches [49], [50], the network is usually constructed by two modules: a *feature extractor* and a *classifier*. Currently, to handle new classes, many works assign a new classifier to the network when a new class emerges [51], [46].

We inherit the concept of feature extractor and classifier, but propose a distinct approach to handle the dynamic label space as shown in Fig. 3. In our case, we use the last full-connection layer as the classifier and the rest as the shared feature extractor (the shared model). In a sense, each neuron in the classifier can be regarded as a learned *prototype* of the corresponding class. Essentially, a *prototype library* is maintained by the clients, which is a table that stores the encountered labels and the corresponding prototypes. Before training starts, a classifier is assembled to build a full model by fetching all the prototypes corresponding to classes present in the training batch. After training on the full model, the classifier is split back into neurons and used to update the prototype library. For prediction, a classifier is built from the whole prototype library. The essential advantage of the prototype library is that it allows direct classification among all seen classes. Moreover, an output neuron will only receive a negative loss and no positive loss if the batch has no samples of its class, which will harm the model’s performance. Our approach mitigates this limitation by only assembling neurons associated with classes present in the batch.

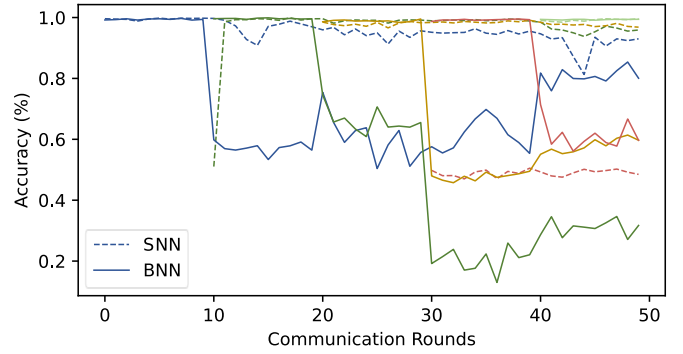
We also adopt the technique of warm-up used in continual learning. When new classes occur, an empty neuron is initialized for it. Classifier containing these neurons is considered *mismatched* with the shared model. Essentially, these empty neurons induce significant loss to the shared model, making parameters in the shared model change dramatically. For the mismatched classifiers, a warm-up is performed before regular training by several epochs of fine-tuning on the batch, freezing the shared model.

By aggregating entries from different tables that have the same label, a global prototype library is obtained. This helps ensemble client knowledge on the classification of the same category. Meanwhile, this also helps share class information with the clients who have yet to encounter a particular class. In addition, the global prototype library can be readily used for prediction.

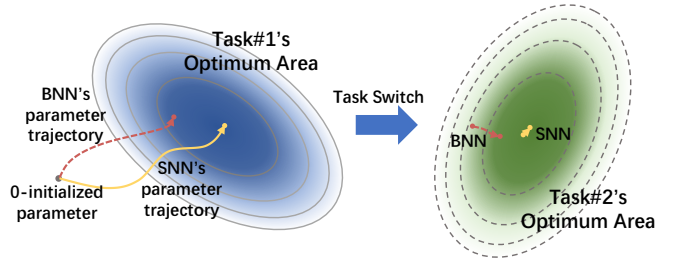
C. SNN Based Initialization

We found that on some small datasets, standard neural network (SNN) tends to exhibit no noticeable performance degradation, whereas BNN suffers from catastrophic forgetting (see Fig. 4a). After in-depth analysis, we ascribe the difference to the effect of prior in BNN. Conventionally, the prior of BNN is set to a 0-centered normal distribution for the sake of simplicity, which suffices for stationary datasets. However, in the case of dynamic distribution, this leads to a problem, as depicted in Fig. 4b.

Previous research on BNN reveals that the prior is a strong regularization for the model, drawing the posterior close to



(a) An example of class-incremental learning on MNIST. The dataset is divided into 5 splits containing number {0,1},{2,3},{4,5},{6,7},{8,9}.



(b) Demonstration of prior’s effect in a simulated 2-D model solution space. Note that on task 1, BNN’s parameter is drawn near the border. Consequently, when switched to task 2, the parameter change is more significant for BNN.

Fig. 4: On small datasets, the performance degradation of BNN is more significant than that of SNN after task switch, due to prior’s effect of BNN.

it. Since the 0-centered prior generally does not lie in the optimum area of the solution space, the BNN is optimized to the optimum area but remains proximal to the border near the prior. Conversely, unconstrained optimization on SNN typically culminates in convergence toward the center of the optimum area. When a slight change in the data distribution happens, the optimum area will drift, so networks are optimized to fit the new distribution. For SNN whose parameter is already located in the center of previous tasks’ optimum area, only small steps are required to fit the new distribution. However, for BNN, whose parameter lies around the border, larger changes are taken to reach the optimum of a changed distribution. Since the change in the parameter is a source of catastrophic forgetting, this explains the observed phenomenon.

Critically, the initial 0-centered prior contains no actual information about data distribution, causing inferior performance than SNN. To overcome this, we suggest the prior initialized from an unconstrained SNN learned from the data distribution. In the probabilistic view, SNN represents the max-a-posteriori (MAP) estimation of the parameter distribution. Consequently, the parameters learned by the SNN serve as a promising initialization for subsequent Bayesian Neural Network (BNN) training endeavors.

Practically, in our algorithm, in the first several rounds, we train an SNN model using the classical FedAvg approach.

Algorithm 1 The FedBNN framework

Input: server, K clients c , local streaming data on each client d_k^r .

Parameter: SNN initialization rounds r_{init} , training parameters.

Output: The global model and prototype library θ^r, H^r .

- 1: Initialize the global model θ^0 as an SNN model, the prototype library H^0 as empty.
 - 2: **while** the system running, round $r = 1, 2, \dots$ **do**
 - 3: Send the model θ^{r-1} and prototype library H^{r-1} to clients.
 - 4: **for** client c_k in all clients **do**
 - 5: Assemble classifier h_k^{r-1} from H^{r-1} .
 - 6: Local model $(\theta|h)_k^r \leftarrow training((\theta|h)^{r-1}, d_k^r)$ via SGD or Bayes by Backprop.
 - 7: Update prototype library H_k^r from head h_k^r .
 - 8: Compute the local likelihood $p(\mathcal{D}_k^T|\theta)$ using Eq.8 if model is BNN.
 - 9: Send local likelihood or local SNN model and prototype library H_k^r to server.
 - 10: **end for**
 - 11: Aggregate using aggregation of FedAvg for SNN or Eq.9 for BNN.
 - 12: Set the prior to global posterior if model is BNN.
 - 13: **if** $r = r_{init}$: Transform θ^r, H^r into BNN models.
 - 14: **end while**
-

Afterward, the server converts the global SNN model into an isomorphic BNN model. The mean of the BNN parameter is set to the corresponding SNN parameter value, and the variance is set to a predetermined value. This distribution is used as the prior and the initial value of the BNN model. In the following rounds, the BNN model is used for training as proposed.

D. Discussion and Limitations

Our approach FedBNN is summarized in Alg. 1. For simplicity, the algorithm assumes full participation for all clients. However, partial participation is allowed by performing local training on selected clients while broadcasting the new global model to all clients. In the paper, we focus on a global prototype library, which may leak local label information in highly privacy sensitive scenarios. In these cases, the prototype library can be kept locally, and only the feature extractor is shared. The local prototype library can also be utilized as a means of personalization[52]. Furthermore, the use of BNN provides uncertainty information about prediction, which is crucial in scenarios like autonomous driving and medical diagnostics [53], [54], [55]. We leave these potential extensions for future research.

V. EXPERIMENTS

A. Experimental Setup

There are currently few approaches designed specifically for FCL problems. Therefore, following existing works on FCL, we implement some continual learning approaches on

top of federated learning frameworks: 1) **Learning without Forgetting (LwF + FL)**, which performs local distillation following the proposal of LwF [23]; 2) **Elastic Weight Consolidation (EWC + FL)**, which regularizes local update with EWC [22]; 3) **Memory Aware Synapse (MAS + FL)**, which regularizes local update with MAS [56]. We also include some federated learning algorithms in the comparison: the vanilla **FedAvg** [57] and **SCAFFOLD** [58], a state-of-art algorithm for heterogeneous federated learning. Since these algorithms cannot deal with dynamic label space by nature, we implement them with the same prototype library as ours. We also include the federated class-incremental learning approach **FCIL** [9] in the experiments on federated class-incremental settings.

The hyperparameters in the experiments are set according to the original proposal or by tuning on the validation set. For a fair comparison, FedBNN uses Bayesian neural network models, and the others use standard neural networks with the same architecture as the BNN. All the experiments are run with 100 participating clients, and 10 of them are selected to participate in each round of training, unless stated otherwise. Detailed experiment settings and further experiment results (standard deviations, experiments with varying participation rates, etc.) are included in the supplementary material.

B. Task-Separate Federated Continual Settings

We first evaluate the performance on the classical task-separate federated continual settings, where all the clients change to some new task simultaneously, while the local distributions across clients are still non-IID (corresponding to Fig. 2a). Specifically, we tested the algorithms with two class-incremental and two task-incremental settings: 1) Class-incremental learning on Cifar-100 [59], split into 4 tasks, each with 25 classes. 2) Class-incremental learning on Tiny-ImageNet [60], split into 4 tasks, each with 50 classes. 3) Task-Incremental classification on small scale images, using Cifar-10 \rightarrow Cifar-100 \rightarrow Tiny-ImageNet. [61], [62], [63]. 4) Task-Incremental classification on larger scale images, using using STL-10 \rightarrow Flowers-102 \rightarrow Food-101 [64], [65], [66].

The accuracy of the compared algorithms is evaluated both at the round of task switch (@TS) and the final round (@Fin), as detailed in Tab. I and Tab. II. It can be observed that the performance of compared baselines varies significantly. While some algorithms (FedAvg, SCAFFOLD) suffer from significant forgetting, some (EWC + FL, MAS + FL) maintains their performance on previous tasks but fail to learn subsequent tasks. This reflects the well-known plasticity-stability dilemma of continual learning [67], [68]. Among the compared baselines, FedBNN demonstrates superior ability in mitigating forgetting while exhibiting comparable adaptability in learning new tasks, consistently reaching the highest average accuracy. Notably, the mere adaptation of continual learning approaches to federated learning settings falls short in effectively addressing the challenges posed by FCL. This highlights the necessity of developing specifically designed algorithms for FCL scenarios.

Cifar-100 Class-Incremental										
Methods	Class Group 1		Class Group 2		Class Group 3		Class Group 4		Average	
	@TS	@Fin	@TS	@Fin	@TS	@Fin	@TS	@Fin	@TS	@Fin
FedAvg	18.86	4.58	25.11	8.93	36.94	8.93	38.50	38.50	29.85	15.23
SCAFFOLD	26.12	17.30	23.77	21.43	38.84	28.91	28.12	28.12	29.21	23.94
EWC + FL	24.91	5.25	17.48	6.81	5.47	7.25	7.70	7.70	13.89	6.75
MAS + FL	15.96	16.07	12.39	13.39	19.42	18.08	20.20	20.20	16.99	16.94
LwF + FL	29.35	5.80	31.47	10.27	42.75	18.42	36.38	36.38	34.99	17.72
FCIL	30.89	22.18	25.27	18.51	36.45	24.12	33.88	33.88	31.62	24.67
FedBNN	33.37	28.73	25.40	21.67	30.95	29.94	30.04	30.04	29.94	27.60

Tiny-ImageNet Class-Incremental										
Methods	Class Group 1		Class Group 2		Class Group 3		Class Group 4		Average	
	@TS	@Fin	@TS	@Fin	@TS	@Fin	@TS	@Fin	@TS	@Fin
FedAvg	9.01	5.79	5.90	2.34	2.12	2.79	2.01	2.01	4.76	3.23
SCAFFOLD	12.72	7.48	13.62	9.15	13.84	10.94	16.18	16.18	14.09	10.94
EWC + FL	4.24	4.02	4.69	5.25	9.15	8.04	8.48	8.48	6.64	6.45
MAS + FL	7.90	5.34	6.01	2.12	2.34	2.79	2.12	2.12	4.59	3.09
LwF + FL	10.95	2.46	17.00	6.03	15.10	13.75	15.88	15.88	14.73	9.53
FCIL	10.69	7.51	14.90	10.37	14.49	13.84	14.34	14.34	13.61	11.50
FedBNN	10.48	7.31	13.52	10.41	16.17	13.75	19.93	19.93	15.02	12.85

TABLE I: The test accuracy (%) of each task at the round of task switch (@TS), and after the final round(@Fin), of the class-incremental settings.

Methods	Small-Scale Image Classification					Large-Scale Image Classification				
	@TS	@Fin	Task 1	Task 2	Task 3	Avg.	Task 1	Task 2	Task 3	Avg.
FedAvg	@TS		10.94	13.84	5.25	10.01	29.13	10.88	5.13	15.04
	@Fin		10.60	4.24	5.25	6.70	9.25	3.98	5.13	6.12
SCAFFOLD	@TS		26.49	4.58	4.00	11.69	37.50	8.25	6.00	17.25
	@Fin		21.92	3.68	4.00	9.87	27.38	7.75	6.00	13.71
EWC+FL	@TS		25.40	2.23	3.78	10.47	32.00	12.75	4.75	16.50
	@Fin		22.54	2.23	3.78	9.52	16.50	6.12	4.75	9.13
MAS+FL	@TS		11.16	11.45	4.56	9.06	12.75	10.88	3.50	9.04
	@Fin		10.60	5.89	4.56	7.02	11.50	4.00	3.50	6.33
LwF+FL	@TS		34.17	15.78	8.26	19.40	33.50	17.87	6.13	19.17
	@Fin		11.27	5.25	8.26	8.26	11.87	4.87	6.13	7.62
FedBNN	@TS		44.45	13.37	8.45	22.09	37.28	14.58	5.91	19.25
	@Fin		22.23	13.09	8.45	14.59	31.83	12.80	5.91	16.85

TABLE II: The test accuracy (%) of each task at the round of task switch (@TS), and after the final round(@Fin), of the task-incremental settings.

C. Gradual Distribution Change

We explore the proposed approach in a more realistic setting, where the task change happens gradually. Specifically, we evaluate the approaches in a class-incremental setting and a task-incremental setting: 1) Gradual federated class-incremental setting, using Tiny-ImageNet, where new classes emerge gradually on clients. 2) Gradual federated task-incremental setting of image classification, using task sequence of Cifar-10 \rightarrow Cifar-100 \rightarrow Tiny-ImageNet.

Tab. III reports the final accuracy of compared algorithms. Similar to results in task-separated settings, FedBNN performs better than the other baselines. Since there are no explicit task boundaries in gradual FCL scenarios, we also propose to measure the performance of algorithms by Focus-on-Now (FON) accuracy curves, as shown in Fig. 5. As the name suggests, the FON curve records model accuracy on *current* global data distribution, which reflects the model performance the user can experience *now* during the system running. It can be found that curves for FedBNN usually lie above the other

baselines, especially during the phase of distribution change. This means that the model for FedBNN adapts well to the current distribution and provides better inference performance for federated continual learning tasks, which is a desirable attribute for real world FCL applications.

VI. CONCLUSION

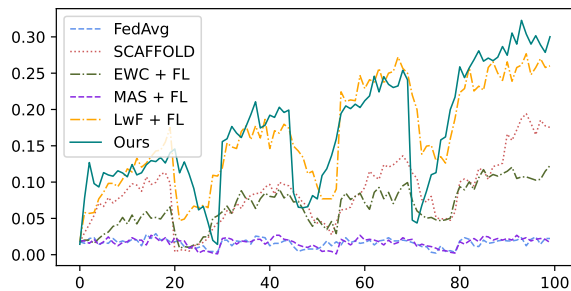
In this paper, we first formulate the problem of Federated Continual Learning, which takes the temporal dynamic of data distribution into consideration beyond classical federated learning. Then, we propose FedBNN to tackle the general FCL challenge. FedBNN utilizes the Bayesian neural network, and integrates knowledge about historical and local distribution into one global model. Through extensive experiments, FedBNN is shown to outperform FL and FCL baselines in various settings.

REFERENCES

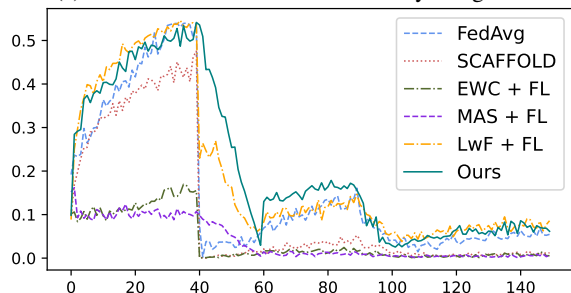
- [1] T. Li, A. K. Sahu, A. Talwalkar, and V. Smith, "Federated learning: Challenges, methods, and future directions," *IEEE Signal Processing Magazine*, vol. 37, no. 3, pp. 50–60, 2020. 1

Methods	Class-Incr, Tiny-ImageNet					Task-Incr, Image Classification			
	Task 1	Task 2	Task 3	Task 4	Avg.	Task 1	Task 2	Task 3	Avg.
FedAvg	2.12	2.01	2.34	2.57	2.26	12.05	3.01	6.70	7.25
SCAFFOLD	8.04	11.94	12.39	19.42	12.95	37.21	5.02	1.56	14.60
EWC+FL	5.47	7.59	7.92	12.72	8.43	17.86	2.34	1.12	7.11
MAS+FL	2.34	2.23	2.34	2.57	2.37	11.05	1.12	0.89	4.35
LwF+FL	6.03	11.83	24.33	27.23	17.35	15.96	8.48	8.93	11.12
FedBNN	8.04	18.28	21.45	30.34	19.53	42.56	15.23	8.29	22.03

TABLE III: The final accuracy (%) under gradual FCL settings.



(a) Gradual class-incremental on Tiny-ImageNet



(b) Gradual task-incremental on image-classification.

Fig. 5: Focus-On-Now (FON) accuracy curves of gradual distribution change settings, which denotes the model accuracy on current data distribution.

- [1] X. Fang and M. Ye, "Robust federated learning with noisy and heterogeneous clients," in *CVPR*. IEEE, 2022, pp. 10072–10081. 1
- [2] A. Hard, K. Rao, R. Mathews, S. Ramaswamy, F. Beaufays, S. Augenstein, H. Eichner, C. Kiddon, and D. Ramage, "Federated learning for mobile keyboard prediction," *arXiv preprint arXiv:1811.03604*, 2018. 1
- [3] S. Ramaswamy, R. Mathews, K. Rao, and F. Beaufays, "Federated learning for emoji prediction in a mobile keyboard," *arXiv preprint arXiv:1906.04329*, 2019. 1
- [4] Q. Yang, J. Zhang, W. Hao, G. P. Spell, and L. Carin, "Flop: Federated learning on medical datasets using partial networks," in *KDD*, 2021, pp. 3845–3853. 1
- [5] S. Samarakoon, M. Bennis, W. Saad, and M. Debbah, "Distributed federated learning for ultra-reliable low-latency vehicular communications," *IEEE Transactions on Communications*, vol. 68, no. 2, pp. 1146–1159, 2019. 1
- [6] T. D. Nguyen, S. Marchal, M. Miettinen, H. Fereidooni, N. Asokan, and A.-R. Sadeghi, "Diot: A federated self-learning anomaly detection system for iot," in *ICDCS*. IEEE, 2019, pp. 756–767. 1
- [7] X. Li, N. Wang, L. Zhu, S. Yuan, and Z. Guan, "Fuse: a federated learning and u-shape split learning-based electricity theft detection framework," *Science China Information Sciences*, vol. 67, no. 4, p. 149302, 2024. 1
- [8] J. Dong, L. Wang, Z. Fang, G. Sun, S. Xu, X. Wang, and Q. Zhu, "Federated class-incremental learning," in *CVPR*, 2022, pp. 10164–10173. 1, 2, 6, 11
- [9] S. Tang, D. Chen, J. Zhu, S. Yu, and W. Ouyang, "Layerwise optimization by gradient decomposition for continual learning," in *CVPR*, 2021, pp. 9634–9643. 1
- [10] M. McCloskey and N. J. Cohen, "Catastrophic interference in connectionist networks: The sequential learning problem," in *Psychology of learning and motivation*. Elsevier, 1989, vol. 24, pp. 109–165. 1
- [11] B. Pfüll and A. Geppert, "A comprehensive, application-oriented study of catastrophic forgetting in dnn," in *ICLR*. OpenReview.net, 2019. 1
- [12] M. Das, X. Chen, X. Yuan, and L. Zhang, "Federated semi-supervised domain adaptation via knowledge transfer," *arXiv preprint arXiv:2207.10727*, 2022. 1
- [13] C. Gong, Z. Zheng, F. Wu, B. Li, Y. Shao, and G. Chen, "Ode: A data sampling method for practical federated learning with streaming data and limited buffer," *arXiv preprint arXiv:2209.00195*, 2022. 1
- [14] Y. Liu, A. Huang, Y. Luo, H. Huang, Y. Liu, Y. Chen, L. Feng, T. Chen, H. Yu, and Q. Yang, "Fedvision: An online visual object detection platform powered by federated learning," in *AAAI*, vol. 34, no. 08, 2020, pp. 13172–13179. 1
- [15] J. Yoon, W. Jeong, G. Lee, E. Yang, and S. J. Hwang, "Federated continual learning with weighted inter-client transfer," in *ICML*, M. Meila and T. Zhang, Eds., vol. 139. PMLR, 2021, pp. 12073–12086. 1, 2
- [16] G. I. Parisi, R. Kemker, J. L. Part, C. Kanan, and S. Wermter, "Continual lifelong learning with neural networks: A review," *Neural Networks*, vol. 113, pp. 54–71, 2019. 2
- [17] M. D. Lange, R. Aljundi, M. Masana, S. Parisot, X. Jia, A. Leonardis, G. G. Slabaugh, and T. Tuytelaars, "A continual learning survey: Defying forgetting in classification tasks," *IEEE Transactions on Pattern Analysis and Machine Intelligence*, vol. 44, no. 7, pp. 3366–3385, 2022. 2
- [18] Q. Yan, D. Gong, Y. Liu, A. van den Hengel, and J. Q. Shi, "Learning bayesian sparse networks with full experience replay for continual learning," in *CVPR*, 2022, pp. 109–118. 2
- [19] L. Wang, K. Yang, C. Li, L. Hong, Z. Li, and J. Zhu, "Ordisco: Effective and efficient usage of incremental unlabeled data for semi-supervised continual learning," in *CVPR*, 2021, pp. 5383–5392. 2
- [20] S. Rebuffi, A. Kolesnikov, G. Sperl, and C. H. Lampert, "iCaRL: Incremental classifier and representation learning," in *CVPR*. IEEE, 2017, pp. 5533–5542. 2
- [21] J. Kirkpatrick, R. Pascanu, N. Rabinowitz, J. Veness, G. Desjardins, A. A. Rusu, K. Milan, J. Quan, T. Ramalho, A. Grabska-Barwinska, D. Hassabis, C. Clopath, D. Kumaran, and R. Hadsell, "Overcoming catastrophic forgetting in neural networks," *Proceedings of the National Academy of Sciences*, vol. 114, no. 13, pp. 3521–3526, 2017. 2, 6
- [22] Z. Li and D. Hoiem, "Learning without forgetting," in *ECCV*, B. Leibe, J. Matas, N. Sebe, and M. Welling, Eds., vol. 9908. Springer, 2016, pp. 614–629. 2, 6
- [23] X. He, J. Sygnowski, A. Galashov, A. A. Rusu, Y. W. Teh, and R. Pascanu, "Task agnostic continual learning via meta learning," *CoRR*, vol. abs/1906.05201, 2019. 2, 3
- [24] C. Zeno, I. Golan, E. Hoffer, and D. Soudry, "Task-agnostic continual learning using online variational bayes with fixed-point updates," *Neural Computation*, vol. 33, no. 11, pp. 3139–3177, 2021. 2
- [25] M. F. Criado, F. E. Casado, R. Iglesias, C. V. Regueiro, and S. Barro, "Non-iid data and continual learning processes in federated learning: A long road ahead," *Information Fusion*, vol. 88, pp. 263–280, 2022. 2
- [26] C. Dupuy, T. G. Roosta, L. Long, C. Chung, R. Gupta, and S. Avestimehr, "Learnings from federated learning in the real world," in *ICASSP*. IEEE, 2022, pp. 8767–8771. 2
- [27] Y. Ma, Z. Xie, J. Wang, K. Chen, and L. Shou, "Continual federated learning based on knowledge distillation," in *Proceedings of the Thirty-First International Joint Conference on Artificial Intelligence, IJCAI 2022, Vienna, Austria, 23-29 July 2022*, L. D. Raedt, Ed. ijcai.org, 2022, pp. 2182–2188. 2
- [28] J. Dong, H. Li, Y. Cong, G. Sun, Y. Zhang, and L. V. Gool, "No one left behind: Real-world federated class-incremental learning," *IEEE Transactions on Pattern Analysis and Machine Intelligence*, vol. 46, no. 4, pp. 2054–2070, 2024. 2

- [30] J. Dong, D. Zhang, Y. Cong, W. Cong, H. Ding, and D. Dai, "Federated incremental semantic segmentation," in *IEEE/CVF Conference on Computer Vision and Pattern Recognition, CVPR 2023, Vancouver, BC, Canada, June 17-24, 2023*. IEEE, 2023, pp. 3934–3943. 2
- [31] Y. Luopan, R. Han, Q. Zhang, C. H. Liu, G. Wang, and L. Y. Chen, "Fedknow: Federated continual learning with signature task knowledge integration at edge," in *39th IEEE International Conference on Data Engineering, ICDE 2023, Anaheim, CA, USA, April 3-7, 2023*. IEEE, 2023, pp. 341–354. 2
- [32] H. Chen, C. Wang, and H. Vikalo, "The best of both worlds: Accurate global and personalized models through federated learning with data-free hyper-knowledge distillation," in *The Eleventh International Conference on Learning Representations, ICLR 2023, Kigali, Rwanda, May 1-5, 2023*. OpenReview.net, 2023. 2
- [33] J. Zhang, Y. Hua, H. Wang, T. Song, Z. Xue, R. Ma, J. Cao, and H. Guan, "GPFL: Simultaneously Learning Global and Personalized Feature Information for Personalized Federated Learning," in *Proceedings of the IEEE/CVF International Conference on Computer Vision, 2023*, pp. 5041–5051. 2
- [34] R. M. Neal, *Bayesian Learning for Neural Networks*. Berlin, Heidelberg: Springer-Verlag, 1996. 2
- [35] C. Blundell, J. Cornebise, K. Kavukcuoglu, and D. Wierstra, "Weight Uncertainty in Neural Network," in *ICML*, vol. 37. JMLR, 2015, pp. 1613–1622. 2
- [36] T. P. Minka, "Expectation propagation for approximate bayesian inference," in *UAI '01: Proceedings of the 17th Conference in Uncertainty in Artificial Intelligence, University of Washington, Seattle, Washington, USA, August 2-5, 2001*, J. S. Breese and D. Koller, Eds. Morgan Kaufmann, 2001, pp. 362–369. 2
- [37] J. Zhao, X. Liu, S. He, and S. Sun, "Probabilistic inference of bayesian neural networks with generalized expectation propagation," *Neurocomputing*, vol. 412, pp. 392–398, 2020. 2
- [38] C. Zhang, J. Bütepage, H. Kjellström, and S. Mandt, "Advances in variational inference," *IEEE Transactions on Pattern Analysis and Machine Intelligence*, vol. 41, no. 8, pp. 2008–2026, 2019. 2
- [39] A. Hubin and G. Storvik, "Variational inference for bayesian neural networks under model and parameter uncertainty," *CoRR*, vol. abs/2305.00934, 2023. 2
- [40] A. Vehtari, S. Särkkä, and J. Lampinen, "On MCMC sampling in bayesian MLP neural networks," in *Proceedings of the IEEE-INNS-ENNS International Joint Conference on Neural Networks, IJCNN 2000, Neural Computing: New Challenges and Perspectives for the New Millennium, Como, Italy, July 24-27, 2000, Volume 1*. IEEE Computer Society, 2000, pp. 317–322. 2
- [41] C. Li, C. Chen, Y. Pu, R. Henao, and L. Carin, "Communication-efficient stochastic gradient MCMC for neural networks," in *The Thirty-Third AAAI Conference on Artificial Intelligence, AAAI 2019, The Thirty-First Innovative Applications of Artificial Intelligence Conference, IAAI 2019, The Ninth AAAI Symposium on Educational Advances in Artificial Intelligence, EAAI 2019, Honolulu, Hawaii, USA, January 27 - February 1, 2019*. AAAI Press, 2019, pp. 4173–4180. 2
- [42] Z. Li, Y. Chen, and F. T. Sommer, "A neural network MCMC sampler that maximizes proposal entropy," *Entropy*, vol. 23, no. 3, p. 269, 2021. 2
- [43] M. Al-Shedivat, J. Gillenwater, E. P. Xing, and A. Rostamizadeh, "Federated learning via posterior averaging: A new perspective and practical algorithms," in *9th International Conference on Learning Representations, ICLR 2021, Virtual Event, Austria, May 3-7, 2021*. OpenReview.net, 2021. 2
- [44] R. Kassab and O. Simeone, "Federated generalized bayesian learning via distributed stein variational gradient descent," *IEEE Trans. Signal Process.*, vol. 70, pp. 2180–2192, 2022. 2
- [45] L. Liu, X. Jiang, F. Zheng, H. Chen, G. Qi, H. Huang, and L. Shao, "A bayesian federated learning framework with online laplace approximation," *IEEE Transactions on Pattern Analysis and Machine Intelligence*, vol. 46, no. 1, pp. 1–16, 2024. 2
- [46] C. V. Nguyen, Y. Li, T. D. Bui, and R. E. Turner, "Variational continual learning," in *ICLR*. OpenReview.net, 2018, p. 18. 2, 5
- [47] C. Zeno, I. Golan, E. Hoffer, and D. Soudry, "Bayesian gradient descent: Online variational bayes learning with increased robustness to catastrophic forgetting and weight pruning," *CoRR*, vol. abs/1803.10123, 2018. 2
- [48] N. Loo, S. Swaroop, and R. E. Turner, "Generalized variational continual learning," in *9th International Conference on Learning Representations, ICLR 2021, Virtual Event, Austria, May 3-7, 2021*. OpenReview.net, 2021. 2
- [49] N. I. Kuo, M. Harandi, N. Fourrier, C. Walder, G. Ferraro, and H. Suominen, "Plastic and stable gated classifiers for continual learning," in *IEEE Conference on Computer Vision and Pattern Recognition Workshops, CVPR Workshops, 2021*, pp. 3553–3558. 5
- [50] K. Chen, H. Lu, R. Wang, and W. Zheng, "Improving class balancing at both feature extractor and classifier head," in *IEEE International Conference on Multimedia and Expo, ICME*. IEEE, 2022, pp. 1–6. 5
- [51] D. Lopez-Paz and M. Ranzato, "Gradient episodic memory for continual learning," in *NeurIPS*, I. Guyon, U. von Luxburg, S. Bengio, H. M. Wallach, R. Fergus, S. V. N. Vishwanathan, and R. Garnett, Eds., 2017, pp. 6467–6476. 5
- [52] A. Z. Tan, H. Yu, L. Cui, and Q. Yang, "Towards personalized federated learning," *IEEE Transactions on Neural Networks and Learning Systems*, pp. 1–17, 2022. 6
- [53] T. Duan, Z. Wang, S. Liu, Y. Yin, and S. N. Srihari, "UNCER: A framework for uncertainty estimation and reduction in neural decoding of EEG signals," *Neurocomputing*, vol. 538, p. 126210, 2023. 6
- [54] A. Vakhitov, L. Ferraz, A. Agudo, and F. Moreno-Noguer, "Uncertainty-aware camera pose estimation from points and lines," in *IEEE Conference on Computer Vision and Pattern Recognition, CVPR 2021, virtual, June 19-25, 2021*. Computer Vision Foundation / IEEE, 2021, pp. 4659–4668. 6
- [55] J. Zhu, X. Ma, and M. B. Blaschko, "Confidence-aware personalized federated learning via variational expectation maximization," in *IEEE/CVF Conference on Computer Vision and Pattern Recognition, CVPR 2023, Vancouver, BC, Canada, June 17-24, 2023*. IEEE, 2023, pp. 24 542–24 551. 6
- [56] R. Aljundi, F. Babiloni, M. Elhoseiny, M. Rohrbach, and T. Tuytelaars, "Memory aware synapses: Learning what (not) to forget," in *ECCV*, vol. 11207. Springer, 2018, pp. 144–161. 6
- [57] B. McMahan, E. Moore, D. Ramage, S. Hampson, and B. A. y Arcas, "Communication-efficient learning of deep networks from decentralized data," in *AISTATS*. PMLR, 2017, pp. 1273–1282. 6
- [58] S. P. Karimireddy, S. Kale, M. Mohri, S. J. Reddi, S. U. Stich, and A. T. Suresh, "SCAFFOLD: stochastic controlled averaging for federated learning," in *ICML*, vol. 119. PMLR, 2020, pp. 5132–5143. 6
- [59] A. Krizhevsky, "Learning multiple layers of features from tiny images," Dept. of Computer Science, Toronto Univ., Technical Report learning-features-2009-TR, 2009. 6, 10
- [60] O. Russakovsky, J. Deng, H. Su, J. Krause, S. Satheesh, S. Ma, Z. Huang, A. Karpathy, A. Khosla, M. Bernstein, A. C. Berg, and L. Fei-Fei, "ImageNet Large Scale Visual Recognition Challenge," *IJCV*, vol. 115, no. 3, pp. 211–252, 2015. 6, 10
- [61] J. J. Hull, "A database for handwritten text recognition research," *IEEE Transactions on Pattern Analysis and Machine Intelligence*, vol. 16, no. 5, pp. 550–554, 1994. 6
- [62] Y. LeCun, L. Bottou, Y. Bengio, and P. Haffner, "Gradient-based learning applied to document recognition," *Proceedings of the IEEE*, vol. 86, no. 11, pp. 2278–2324, 1998. 6
- [63] G. Cohen, S. Afshar, J. Tapson, and A. van Schaik, "EMNIST: extending MNIST to handwritten letters," in *IJCNN*. IEEE, 2017, pp. 2921–2926. 6
- [64] A. Coates, A. Y. Ng, and H. Lee, "An analysis of single-layer networks in unsupervised feature learning," in *AISTATS*, G. J. Gordon, D. B. Dunson, and M. Dudik, Eds., vol. 15. JMLR, 2011, pp. 215–223. 6, 10
- [65] M. Nilsback and A. Zisserman, "Automated flower classification over a large number of classes," in *ICVGIP*. IEEE, 2008, pp. 722–729. 6, 10
- [66] L. Bossard, M. Guillaumin, and L. V. Gool, "Food-101 - Mining Discriminative Components with Random Forests," in *ECCV*, vol. 8694. Springer, 2014, pp. 446–461. 6, 10
- [67] W. C. Abraham and A. Robins, "Memory retention – the synaptic stability versus plasticity dilemma," *Trends in Neurosciences*, vol. 28, no. 2, pp. 73–78, 2005. 6
- [68] D. Jung, D. Lee, S. Hong, H. Jang, H. Bae, and S. Yoon, "New insights for the stability-plasticity dilemma in online continual learning," *CoRR*, vol. abs/2302.08741, 2023. 6
- [69] T. H. Hsu, H. Qi, and M. Brown, "Measuring the effects of non-identical data distribution for federated visual classification," *CoRR*, vol. abs/1909.06335, 2019. 11

APPENDIX A
DETAILED ALGORITHM

In this section, we present a more detailed description of the proposed FedBNN algorithm (Alg. 2). The loop continues until the system stops running, but at any time, the latest head library and shared model can be used to perform inference on the server or clients. For the sake of simplicity, the algorithm assumes full participation for all clients. However, partial participation is allowed by performing local training on selected clients, while broadcasting new global model to all clients.

Algorithm 2 FedBNN

Input: server, K clients c , local streaming data on each client d_k^r .

Parameter: SNN initialization rounds r_{init} , training parameters.

Output: The global model and prototype library for prediction θ^r, H^r

- 1: Initialize the global model θ^0 as an SNN model, the prototype library H^0 as empty.
 - 2: **while** the system running, round $r = 1, 2, \dots$ **do**
 - 3: Send the model θ^{r-1} and prototype library H^{r-1} to clients.
 - 4: **for** client c_k in all clients **do**
 - 5: Client training using Alg. 3.
 - 6: **end for**
 - 7: Server aggregation using Alg. 4.
 - 8: **if** $r = r_{init}$ **then**
 - 9: Transform θ^r, H^r into BNN models.
 - 10: **end if**
 - 11: **end while**
-

Algorithm 3 Client training

Input: Global model and prototype library of last round θ^{r-1}, H^{r-1}

- 1: Assemble classifier h_k^{r-1} from H^{r-1} .
 - 2: **if** local model is SNN **then**
 - 3: Local model $(\theta|h)_k^r \leftarrow training((\theta|h)^{r-1}, d_k^r)$ via SGD.
 - 4: Update prototype library H_k^r from head h_k^r .
 - 5: Send local model θ_k^r and prototype library H_k^r to server.
 - 6: **else**
 - 7: Local model $(\theta|h)_k^r \leftarrow training((\theta|h)^{r-1}, d_k^r)$ via Bayes by Backprop.
 - 8: Update prototype library H_k^r from head h_k^r .
 - 9: Calculate the likelihood by Eq.8.
 - 10: Send local likelihood $p(D_k^T|\theta)$ and prototype library H_k^r to server.
 - 11: **end if**
-

APPENDIX B
DETAILED EXPERIMENTAL SETUP

In this section, we elaborate the details of experiments, including datasets and hyper-parameters. All the experiments

Algorithm 4 Server aggregation

Input: local prototype libraries H_k^r , local models θ_k^r or local likelihood $\{p(D_k^T|\theta)\}$ and latest global model θ^{r-1} .

Output: The aggregated global model and prototype library θ^r, H^r

- 1: Aggregate the prototype library $H^r \leftarrow agg(\{H_k^r\})$.
 - 2: **if** local models are SNN **then**
 - 3: Aggregate using aggregation of FedAvg : $\theta^r \leftarrow agg(\{\theta_k^r\})$.
 - 4: **else**
 - 5: Aggregate using Equation 9 : $\theta^r \leftarrow agg(\theta^{r-1}, \{p(D_k^T|\theta)\})$.
 - 6: **end if**
-

are deployed on a x86_64 server with 2x Intel 40-core CPUs, 160GB memory, and 2x NVIDIA RTX3090 GPUs.

A. Datasets

Cifar-10 [59] is a popular image classification benchmark dataset, which consists of 60,000 colored images with the resolution of 32x32, covering 10 classes, with 6,000 images per class. The dataset is divided into a training set of 50,000 samples and a test set of 10,000 samples.

Cifar-100 [59] is an extension of Cifar-10, which contains 100 classes. Each class contains 500 training samples and 100 test samples.

Tiny-ImageNet is an image classification dataset extracted from ImageNet dataset [60]. It contains 200 selected classes, each with 500 training images, 50 validating images and 50 test images. All the samples are 64x64 colored images. In the class-incremental experiment, the original images are used. In the task-incremental experiment, the samples are resized to 32x32 colored images to match the dimension of Cifar-10 and Cifar-100.

STL-10 [64] is an image recognition dataset inspired by Cifar-10 dataset with some improvements. The dataset contains 10 classes with 500 training samples and 800 test samples per class. The samples are 96x96 pixel colored images.

Flowers-102 (Oxford 102 flowers) [65] dataset is a consistent of 102 flower categories commonly occurring in the United Kingdom. The training and test set consist of 6,149 and 1020 colored images respectively. The images have large scale, pose and light variations. In addition, there are categories that have large variations within the category and several very similar categories. In the task-incremental experiment, the samples are resized to 96x96 images to match the dimension with other tasks.

Food-101 [66] is an image classification dataset consisting of 101 food categories. For each class, 750 training samples are provided as well as 250 test samples. On purpose, the training images were not cleaned, and thus still contain some amount of noise. In the task-incremental experiment, the samples are resized to 96x96 colored images to match the dimension with other tasks.

B. Data Generation Strategy

To simulate the complicated data evolution patterns of the various FCL cases discussed in the paper, we implement an

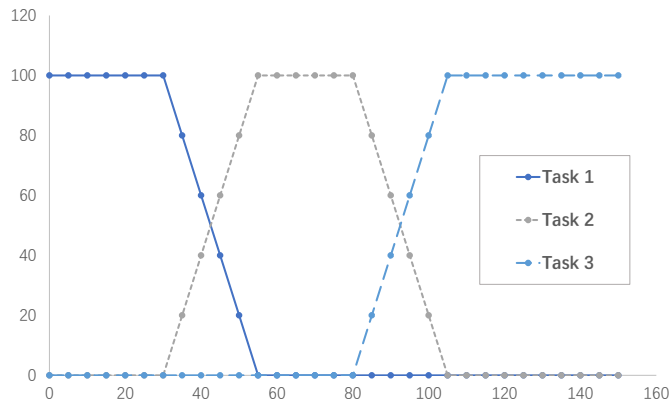


Fig. 6: Task switch pattern in the gradual FCL Setting. The vertical axis is the data proportion of each task, measured in percentage; the horizontal axis is the communication rounds.

FCL data generation simulator for the experiments. Here, we describe each of the data generation strategies used in the different experiment settings.

Task Separate FCL Setting In the task separate class-incremental and task-incremental setting, class groups and datasets are used as tasks respectively. Each task spans several rounds, while switch to the next task happens at certain rounds, known as task boundaries. The task samples are used as the global data during the rounds of each task. To simulate the non-IID characteristic of client data, global data are partitioned based on Dirichlet distribution into client datasets, as described in [69]. The task boundaries of each setting tested in our experiment is listed in Tab. IV.

Gradual FCL Setting In this setting, each task is assigned with a period of rounds as their duration. The duration of each task overlaps with previous and following tasks. During overlapped rounds, global data is formed by samples from the two tasks. The proportion of the previous task will gradually decrease while samples from the next task will increase, as depicted in Fig. 6. To simulate the behavior that some clients change to the new task first, we first decide the number of clients for each task, corresponding to the task proportion. Then the task data is partitioned based on Dirichlet non-IID among the clients. The duration of each tasks in our experiment is listed in Tab. V.

C. Implementation Detail

Algorithm Implementation In the experiment, we implemented FedBNN and the baselines FedAvg, SCAFFOLD, EWC + FL, MAS + FL, and LwF + FL. All the implementations are based on the PyTorch 1.12 machine learning framework³. For FedBNN, we choose torchbnn⁴ as the Bayesian neural network library. All the baselines are carefully implemented based on the original paper and reference source codes provided by the authors.

For the FCIL baseline [9], we used the source code provided by the author⁵. We made proper modification to the source

code regarding data generation and evaluation to match with other compared algorithms.

Model Architecture In the paper, we use ResNet-18 for all the experiments and all the baselines. The detailed network architecture is specified in Tab. VI, while the structure of residual layer is demonstrated in Tab. VII.

APPENDIX C FURTHER EXPERIMENT RESULTS

In this section, we further present some empirical results of FedBNN and the compared baselines. The experiment settings are consistent with experiments in the main paper and the previous section.

A. Task-Separate Federated Continual Settings

Due to page limitations, the standard deviation of numerical results are not reported in the main paper. In this section, we present the standard deviations of the results under task-separate FCL settings. Tab. VIII corresponds to Tab. I in the main paper, while Tab. IX corresponds to Tab. II.

B. Gradual Distribution Change

Due to page limitations, the standard deviation of numerical results are not reported in the main paper. In this section, we present the standard deviations of the results under gradual FCL settings. Tab. X corresponds to Tab. III in the main paper.

C. Effect of Participation Ratio

In the main paper, we use 100 clients in total, and select 10 clients at each round for training, i.e. the participation ratio is set to 0.1. To better understand the effect of different participation ratios, we scale the participation ratio in between 0.1 and 0.6 and conduct further experiments. Specifically, we choose 10, 20, 40, 60 clients out of total 100 clients to obtain results with participation ratio 0.1, 0.2, 0.4, 0.6. We run the experiment under the class-incremental Tiny-ImageNet setting and the task-incremental small-scale image-classification setting.

Fig. 7 presents the accuracy of the compared baselines with regard to different participation ratios. It can be observed that while some baselines (MAS + FL and EWC + FL) are less sensitive to participation ratio, most algorithms see improvements in terms of accuracy with increasing participation ratio. Furthermore, FedBNN consistently outperform the baselines with different participation ratios, which demonstrates the effectiveness of our approach.

³Project homepage: <https://pytorch.org/>

⁴Project repository: <https://github.com/Harry24k/bayesian-neural-network-pytorch>

⁵Project repository: <https://github.com/conditionWang/FCIL>

TABLE IV: The task boundaries of tested settings in the experiment.

Experiment Setting	Task Boundaries (Round#)
Cifar-100 Class-Incremental	4 tasks each with 25 classes: 25,50,75,100
Tiny-ImageNet Class-Incremental	4 tasks each with 50 classes: 25,50,75,100
Small-Scale Object Classification	3 tasks: 50,100,150
Larger-Scale Object Classification	3 tasks: 50,100,150

TABLE V: The task duration of tested gradual FCL settings in the experiment.

Setting	Task	Task Duration (Rounds#)
Tiny-ImageNet Gradual Class-Incremental	Class Group 1	0-30
	Class Group 2	20-55
	Class Group 3	45-80
	Class Group 4	70-100
Obj-Classification Gradual Task-Incremental	Cifar-10	0 - 60
	Cifar-100	40 - 110
	Tiny-ImageNet	90 - 150

TABLE VI: Architecture of ResNet-18 model used in our experiment.

Layer name	Description
conv1	Conv2d layer, $3 \rightarrow 64$ channels, 7×7 kernel, stride 4, padding 1, with BatchNorm, ReLU and 3×3 MaxPooling (matches input dimension)
res1	Residual layer, $64 \rightarrow 64$ channels, stride 1
res2	Residual layer, $64 \rightarrow 128$ channels, stride 2
res3	Residual layer, $128 \rightarrow 256$ channels, stride 2
res4	Residual layer, $256 \rightarrow 512$ channels, stride 2
fc1	Linear layer, $[n_{res4_out}, 1000]$ with ReLU (Matches res4 output dimension)
classifier	Linear layer, $[1000, n_{class}]$ with SoftMax (Matches output classes)

TABLE VII: Architecture of residual layer in the ResNet-18 model.

Layer name	Description
conv1	Conv2d layer, $n_{in} \rightarrow n_{out}$ channels, 3×3 kernel, stride n_{stride} , padding 1, no bias, with BatchNorm and ReLU.
conv2	Conv2d layer, $n_{out} \rightarrow n_{out}$ channels, 3×3 kernel, stride 1, padding 1, no bias, with BatchNorm.
downsample	Conv2d layer, present if $n_{stride} \neq 1$ or $n_{in} \neq n_{out}$, $n_{in} \rightarrow n_{out}$ channels, 3×3 kernel, stride n_{stride} , padding 1, no bias, with BatchNorm.
Computation	$output = conv2(conv1(input)) + downsample(input)$

Cifar-100 Class-Incremental												
Methods	Class Group 1		Class Group 2		Class Group 3		Class Group 4		Average			
	@TS	@Fin	@TS	@Fin	@TS	@Fin	@TS	@Fin	@TS	@Fin		
FedAvg	18.86 ± 0.90	4.58 ± 0.17	25.11 ± 0.06	8.93 ± 0.23	36.94 ± 0.94	8.93 ± 0.13	38.50 ± 1.81	38.50 ± 1.81	29.85 ± 0.43	15.23 ± 0.40		
SCAFFOLD	26.12 ± 1.05	17.30 ± 0.85	23.77 ± 1.71	21.43 ± 0.88	38.84 ± 2.11	28.91 ± 1.24	28.12 ± 0.86	28.12 ± 0.86	29.21 ± 0.59	23.94 ± 0.20		
EWC + FL	24.91 ± 0.52	5.25 ± 0.04	17.48 ± 0.63	6.81 ± 0.56	5.47 ± 0.29	7.25 ± 0.25	7.70 ± 0.01	7.70 ± 0.01	13.89 ± 0.35	6.75 ± 0.10		
MAS + FL	15.96 ± 0.98	16.07 ± 0.76	12.39 ± 0.66	13.39 ± 0.88	19.42 ± 0.60	18.08 ± 1.25	20.20 ± 0.49	20.20 ± 0.49	16.99 ± 0.28	16.93 ± 0.23		
LwF + FL	29.35 ± 2.27	5.80 ± 0.18	31.47 ± 0.31	10.27 ± 1.29	42.75 ± 0.36	18.42 ± 0.56	36.38 ± 0.53	36.38 ± 0.53	34.99 ± 0.52	17.72 ± 0.30		
FCIL	30.89 ± 0.14	22.18 ± 0.82	25.27 ± 1.00	18.51 ± 2.01	36.45 ± 1.14	24.12 ± 0.68	33.88 ± 0.62	33.88 ± 0.62	31.62 ± 0.40	24.67 ± 1.00		
FedBNN	33.37 ± 0.59	28.73 ± 0.37	25.40 ± 0.91	21.67 ± 1.27	30.95 ± 0.85	29.94 ± 1.31	30.04 ± 0.75	30.04 ± 0.75	29.94 ± 0.32	27.59 ± 0.60		

Tiny-ImageNet Class-Incremental												
Methods	Class Group 1		Class Group 2		Class Group 3		Class Group 4		Average			
	@TS	@Fin	@TS	@Fin	@TS	@Fin	@TS	@Fin	@TS	@Fin		
FedAvg	9.01 ± 0.23	5.79 ± 0.20	5.90 ± 0.24	2.34 ± 0.09	2.12 ± 0.11	2.79 ± 0.09	2.01 ± 0.34	2.01 ± 0.34	4.76 ± 0.11	3.23 ± 0.14		
SCAFFOLD	12.72 ± 1.61	7.48 ± 0.24	13.62 ± 0.57	9.15 ± 0.26	13.84 ± 0.34	10.94 ± 0.47	16.18 ± 1.26	16.18 ± 1.26	14.09 ± 0.44	10.94 ± 0.16		
EWC + FL	4.24 ± 0.07	4.02 ± 0.29	4.69 ± 0.03	5.25 ± 0.46	9.15 ± 0.18	8.04 ± 0.29	8.48 ± 0.43	8.48 ± 0.43	6.64 ± 0.06	6.45 ± 0.06		
MAS + FL	7.90 ± 0.33	5.34 ± 0.11	6.01 ± 0.16	2.12 ± 0.27	2.34 ± 0.14	2.79 ± 0.30	2.12 ± 0.01	2.12 ± 0.01	4.59 ± 0.16	3.09 ± 0.17		
LwF + FL	10.95 ± 0.65	2.46 ± 0.09	17.00 ± 0.35	6.03 ± 0.21	15.10 ± 1.09	13.75 ± 2.11	15.88 ± 1.23	15.88 ± 1.23	14.73 ± 0.40	9.53 ± 0.19		
FCIL	10.69 ± 0.78	7.51 ± 0.03	14.90 ± 1.60	10.37 ± 0.79	14.49 ± 1.74	13.84 ± 0.10	14.34 ± 0.78	14.34 ± 0.78	13.60 ± 0.44	11.52 ± 0.36		
FedBNN	10.48 ± 0.58	7.31 ± 0.32	13.52 ± 0.43	10.41 ± 0.79	16.17 ± 1.47	13.75 ± 0.44	19.93 ± 0.26	19.93 ± 0.26	15.03 ± 0.40	12.85 ± 0.24		

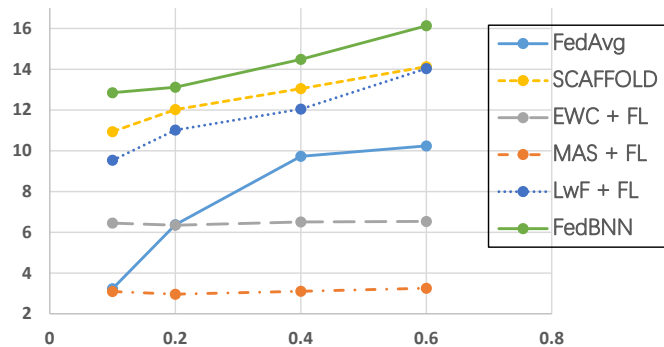
TABLE VIII: The test accuracy (%) of each task at the round of task switch (@TS), and after the final round(@Fin), of the class-incremental settings.

Methods		Small-Scale Image Classification					Large-Scale Image Classification				
		Task 1	Task 2	Task 3	Avg.	Task 1	Task 2	Task 3	Avg.		
FedAvg	@TS	10.94 ± 0.84	13.84 ± 0.71	5.25 ± 0.44	10.01 ± 0.20	29.13 ± 0.68	10.88 ± 0.16	5.13 ± 0.12	15.05 ± 0.32		
	@Fin	10.60 ± 2.45	4.24 ± 0.41	5.25 ± 0.44	6.70 ± 0.54	9.25 ± 0.12	3.98 ± 0.13	5.13 ± 0.12	6.12 ± 0.05		
SCAFFOLD	@TS	26.49 ± 0.56	4.58 ± 0.16	4.00 ± 0.08	11.69 ± 0.26	37.50 ± 1.45	8.25 ± 0.17	6.00 ± 0.07	17.25 ± 0.56		
	@Fin	21.92 ± 0.54	3.68 ± 0.17	4.00 ± 0.08	9.87 ± 0.25	27.38 ± 2.19	7.75 ± 0.05	6.00 ± 0.07	13.71 ± 0.76		
EWC+FL	@TS	25.40 ± 0.17	2.23 ± 0.19	3.78 ± 0.17	10.47 ± 0.16	32.00 ± 1.43	12.75 ± 1.21	4.75 ± 0.13	16.50 ± 0.91		
	@Fin	22.54 ± 1.78	2.23 ± 0.21	3.78 ± 0.17	9.52 ± 0.70	16.50 ± 0.99	6.12 ± 0.21	4.75 ± 0.13	9.12 ± 0.34		
MAS+FL	@TS	11.16 ± 0.65	11.45 ± 0.28	4.56 ± 0.11	9.06 ± 0.33	12.75 ± 0.84	10.88 ± 0.99	3.50 ± 0.17	9.04 ± 0.58		
	@Fin	10.60 ± 0.87	5.89 ± 0.15	4.56 ± 0.11	7.02 ± 0.31	11.50 ± 0.65	4.00 ± 0.22	3.50 ± 0.17	6.33 ± 0.15		
LwF+FL	@TS	34.17 ± 1.38	15.78 ± 0.59	8.26 ± 0.18	19.40 ± 0.59	33.50 ± 2.08	17.87 ± 0.14	6.13 ± 0.24	19.17 ± 0.68		
	@Fin	11.27 ± 1.06	5.25 ± 0.40	8.26 ± 0.18	8.26 ± 0.48	11.87 ± 0.93	4.87 ± 0.16	6.13 ± 0.24	7.62 ± 0.30		
FedBNN	@TS	44.45 ± 1.02	13.37 ± 0.73	8.45 ± 0.15	22.09 ± 0.53	37.28 ± 1.55	14.58 ± 0.91	5.91 ± 0.32	19.26 ± 0.11		
	@Fin	22.23 ± 1.24	13.09 ± 1.03	8.45 ± 0.15	14.59 ± 0.71	31.83 ± 1.46	12.80 ± 2.34	5.91 ± 0.32	16.85 ± 1.30		

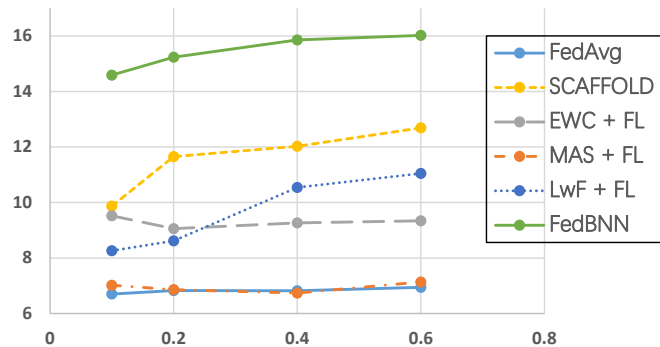
TABLE IX: The test accuracy (%) of each task at the round of task switch (@TS), and after the final round(@Fin), of the task-incremental settings.

Methods	Class-Incr, Tiny-ImageNet					Task-Incr, Image Classification				
	Task 1	Task 2	Task 3	Task 4	Avg.	Task 1	Task 2	Task 3	Avg.	
FedAvg	2.12 ± 0.15	2.01 ± 0.14	2.34 ± 0.07	2.57 ± 0.09	2.26 ± 0.07	12.05 ± 0.99	3.01 ± 0.25	6.70 ± 0.12	7.25 ± 0.29	
SCAFFOLD	8.04 ± 0.32	11.94 ± 1.96	12.39 ± 0.76	19.42 ± 1.22	12.95 ± 0.89	37.21 ± 0.82	5.02 ± 0.25	1.56 ± 0.34	14.60 ± 0.45	
EWC+FL	5.47 ± 0.08	7.59 ± 0.38	7.92 ± 0.13	12.72 ± 0.80	8.43 ± 0.23	17.86 ± 0.34	2.34 ± 0.08	1.12 ± 0.26	7.11 ± 0.17	
MAS+FL	2.34 ± 0.06	2.23 ± 0.09	2.34 ± 0.18	2.57 ± 0.54	2.37 ± 0.16	11.05 ± 1.43	1.12 ± 0.28	0.89 ± 0.13	4.35 ± 0.48	
LwF+FL	6.03 ± 0.06	11.83 ± 0.35	24.33 ± 1.49	27.23 ± 0.02	17.36 ± 0.35	15.96 ± 0.60	8.48 ± 0.33	8.93 ± 0.22	11.12 ± 0.25	
FedBNN	8.04 ± 0.33	18.28 ± 1.34	21.45 ± 2.20	30.34 ± 1.39	19.53 ± 0.46	42.56 ± 1.20	15.23 ± 2.15	8.29 ± 0.10	22.03 ± 0.80	

TABLE X: The final accuracy (%) under gradual FCL settings.



(a) Average final accuracy of class-incremental FCL setting on Tiny-ImageNet. X-axis is the participation ratio, and Y-axis is accuracy (%).



(b) Average final accuracy of task-incremental FCL setting on small-scale image classification. X-axis is the participation ratio, and Y-axis is accuracy (%).

Fig. 7: Average final accuracy of the algorithms with varying participation ratio.